PIER Letters

(Received 29 November 2024, Accepted 9 January 2025, Scheduled 20 January 2025)

Credibility Assessment of EMC Uncertainty Analysis Based on Failure Rate

Shenghang Huo, Zhengyu Xue*, Yuhan Zhou, Jinming Yao, and Jinjun Bai

College of Marine Electrical Engineering, Dalian Maritime University, Dalian 116026, China

ABSTRACT: Uncertainty analysis has been widely used in electromagnetic compatibility (EMC) simulation. However, a comprehensive credibility assessment system for it has yet to be established. In this article, the concepts of failure domain and failure rate are introduced from the perspective of the practical application of uncertainty analysis methods. The study aims to assess the reliability of uncertainty analysis method from the perspective of system failure, providing a theoretical basis for guiding practical electromagnetic compatibility design through uncertainty analysis.

1. INTRODUCTION

For deterministic EMC simulations, credibility assessment has reached a relatively mature stage. In 2008, the IEEE Standards Association introduced the 1597.1 standard, titled "IEEE Standard for Validation of Computational Electromagnetics Computer Modeling and Simulations" [1], along with detailed implementation guidance [2]. The standard takes Feature Selection Validation (FSV) method as a core step to quantitatively evaluate the difference between simulation results and standard results, avoiding the subjectivity and non-transmissibility of human judgment. In recent years, FSV method has been improved in terms of computational performance and applicability. Orlandi et al. introduced 2D-FSV, which applies 2D Fourier Transform to extend the method for the credibility assessment of 2D simulation models [3]. Zhang et al. introduced a continuous probability density distribution function into the evaluation results of FSV method to obtain more easily interpretable results [4]. They also proposed using the low-frequency component of the data as a reference to address the issues of the FSV method in the credibility assessment of over-zero data. Zhang et al. proposed extending the FSV method to multidimensional simulation model credibility assessment through an iterative approach [5]. In 2022, the IEEE Standards Association revised the 1597.1 standard to incorporate various improvements [6].

In recent years, uncertainty analysis has been developed into a comprehensive research framework in the field of EMC [7, 8]. Uncertainty factors in the actual electromagnetic environment introduce randomness into the inputs. To ensure the reliability and practicality of electromagnetic protection design, uncertainty analysis method is introduced to study the impact of these uncertainty factors on electromagnetic design.

To fill the gap in the uncertainty EMC simulation evaluation system, Jauregui et al. improved FSV method and successfully applied it to EMC uncertainty simulation evaluation [9]. FSV can quantitatively assess the accuracy of uncertainty analysis methods. Ferson et al. introduced the area metric and probability integral transform to calculate the area difference between the probability distribution functions of the output response from the model and reference result [10]. Bai et al. introduced Mean Equivalent Area Method (MEAM) to replace the probability density function with a uniform distribution for ease of calculation, using the equivalent area to evaluate the performance of the uncertainty analysis method [11].

However, in existing studies on EMC uncertainty analysis, the mean value, standard deviation, and root mean square error are often used as evaluation criteria [12]. While these metrics provide an overall assessment of the uncertainty analysis method's performance, they fail to account for system failures caused by uncertainty factors in practical engineering. In practical engineering, the system's input fluctuates within an uncertainty interval, which in turn causes a large fluctuation range in the output, which may even cross the critical failure value, resulting in failure. For example, the uncertainty in the aperture size of the electromagnetic shielding box can affect the shielding effectiveness. Certain equipment requires the shielding effectiveness to meet a specific threshold to ensure proper operation within the shielding box. If the shielding effectiveness falls below this threshold, it is deemed a failure. Therefore, the failure rate can also serve as an evaluation criterion for EMC uncertainty analysis, enhancing the reliability and practicality of electromagnetic design.

With the development of machine learning, uncertainty analysis methods based on surrogate models have become a popular research topic [13]. Kriging and LSSVR are representative methods. Therefore, this article applies Kriging and LSSVR methods to perform uncertainty analysis on the shielding effectiveness example of a metal box to obtain failure rate results. Monte Carlo Method (MCM) is used as a reference, and

* Corresponding author: Zhengyu Xue (xuezy@dlmu.edu.cn).

a credibility assessment method based on failure rate is applied to compare the accuracies of Kriging and LSSVR.

This article is structured as follows. Section 2 introduces three uncertainty analysis methods: MCM, Kriging, and LSSVR. In Section 3, the concepts of failure domain and failure rate are introduced. Section 4 applies the Robinson method and finite element method to two metal box shielding effectiveness examples to test the performance of failure rate. Section 5 summarizes the article.

2. UNCERTAINTY ANALYSIS METHODS

When dealing with uncertainty analysis, a random variable model in vector form is usually used to describe uncertainty factors, as follows:

$$\boldsymbol{\xi} = \{\xi_1, \xi_2, \ldots, \xi_j, \ldots, \xi_N\} \tag{1}$$

where ξ_j is a random variable, $\boldsymbol{\xi}$ a vector of random variables, and N the number of random variables.

2.1. MCM

The principle of MCM is to characterize a random variable $\boldsymbol{\xi}$ by using exhaustive sampling points $\mathbf{S}_1 = [\mathbf{X}_1, \mathbf{X}_2, \ldots, \mathbf{X}_n]$, meaning that all possible scenarios are considered, where the number of sampling points is denoted as n, and each sampling point $\mathbf{X}_i$ is an N-dimensional vector, as follows:

$$\mathbf{X}_i = \{X_i(1), X_i(2), \ldots, X_i(j), \ldots, X_i(N)\} \tag{2}$$

where $X_i(j)$ are all determined constant values that correspond to ξ_j in Equation (1).

The MCM-based approach to EMC uncertainty analysis involves performing deterministic EMC simulations at each sampling point $\mathbf{X}_i$.

$$\mathbf{Y}_i = \mathrm{EMC}[\mathbf{X}_i] \tag{3}$$

where EMC[ ] represents a single deterministic EMC simulation process. $\mathbf{Y}_i$ is the result of a single EMC simulation, and its dimension is not N. It must be specifically determined based on the output of interest. $\mathbf{Y} = [\mathbf{Y}_1, \mathbf{Y}_2, \ldots, \mathbf{Y}_n]$ is the set of EMC simulation results, i.e., MCM-based simulation results. The data is then statistically analyzed to obtain the results of the uncertainty analysis. In this article, the uncertainty analysis results from MCM serve as the reference standard.

2.2. Uncertainty Analysis Methods Based on the Surrogate Model

When a problem that requires significant computational effort and is difficult to solve is encountered in practical engineering, the original model can be replaced by a simplified model with lower computational requirements and faster solution speed. This simplified model is called a surrogate model.

First, the sampling space is sampled, for example, using Latin hypercube sampling to obtain m sampling points ($\mathbf{S}_2 = [\mathbf{x}_1, \mathbf{x}_2, \ldots, \mathbf{x}_m]$), where m is significantly smaller than n. $\mathbf{x}_i$ is also an N-dimensional constant value vector data. Deterministic EMC simulation is performed at each sampling point $\mathbf{x}_i$.

$$\mathbf{y}_i = \mathrm{EMC}[\mathbf{x}_i] \tag{4}$$

$\mathbf{y} = [\mathbf{y}_1, \mathbf{y}_2, \ldots, \mathbf{y}_m]^{\mathrm{T}}$ is the set of EMC simulation results. The training set $\{\mathbf{x}_i, \mathbf{y}_i\}_{i=1}^m$ is obtained from the above analysis and is used to train surrogate models.

Here, the two surrogate models used in this article, Kriging and LSSVR, are introduced.

Kriging model is an interpolation model that generates interpolated results by linearly weighting the known EMC simulation results, $\mathbf{y}_i$.

$$\hat{y}(\mathbf{x}) = \sum_{i=1}^{m} w_i y_i \tag{5}$$

where $\mathbf{w} = [w_1, w_2, \ldots, w_m]^{\mathrm{T}}$ are the weighting coefficients, and by assigning the value of the weighting coefficients $\mathbf{w}$, the response value of any point in the sampling space can be obtained.

As concluded in [14], Kriging model can be ultimately expressed as:

$$\hat{y}(\mathbf{x}) = \beta_0 + \mathbf{r}^{\mathrm{T}}(\mathbf{x})\mathbf{R}^{-1}\left(\mathbf{y} - \beta_0\mathbf{F}\right) \tag{6}$$

where $\beta_0 = (\mathbf{F}^{\mathrm{T}}\mathbf{R}^{-1}\mathbf{F})^{-1}\mathbf{F}^{\mathrm{T}}\mathbf{R}^{-1}\mathbf{y}$, $\mathbf{F} = [1,\ 1,\ \ldots,\ 1]^{\mathrm{T}}$, $\mathbf{R} = \begin{bmatrix} R(\mathbf{x}_1, \mathbf{x}_1) & \cdots & R(\mathbf{x}_1, \mathbf{x}_m) \\ \vdots & & \vdots \\ R(\mathbf{x}_m, \mathbf{x}_1) & \cdots & R(\mathbf{x}_m, \mathbf{x}_m) \end{bmatrix}$, and $\mathbf{r} = \begin{bmatrix} R(\mathbf{x}_1, \mathbf{x}) \\ \vdots \\ R(\mathbf{x}_m, \mathbf{x}) \end{bmatrix}$.

Let $\mathbf{V}_{\mathrm{krig}} = \mathbf{R}^{-1}\left(\mathbf{y} - \beta_0\mathbf{F}\right)$, then both β_0 and $\mathbf{V}_{\mathrm{krig}}$ are related only to known sample points.

Finally, Kriging is used to calculate the response values of all the sampling points in the exhaustive sampling space $\mathbf{S}_1$, resulting in the set of Kriging-based simulation results $\mathbf{Y}_{\mathrm{krig}}$. They are then aggregated to obtain the results of the uncertainty analysis.

LSSVR is also a commonly used surrogate model in EMC uncertainty analysis, with the advantages of fast training, good generalization, and the ability to fit nonlinear functions.

LSSVR maps the input space to a high-dimensional feature space via a nonlinear mapping $\phi(\cdot)$ and identifies the optimal linear function within this feature space. The dimension of the high-dimensional feature space may be infinite, and the specific form of the nonlinear mapping $\phi(\cdot)$ is typically unknown. Therefore, the kernel function technique in Equation (7) is employed to significantly simplify the computation by replacing the direct calculation of the nonlinear mapping with its inner product.

$$K(\mathbf{x}_i, \mathbf{x}_j) = \phi(\mathbf{x}_i) \cdot \phi(\mathbf{x}_j) \tag{7}$$

where $K(\mathbf{x}_i, \mathbf{x}_j)$ is the kernel function, and in this paper the Gaussian kernel function $K(\mathbf{x}_i, \mathbf{x}_j) = \exp(-\parallel \mathbf{x}_i - \mathbf{x}_j \parallel^2 / \rho^2)$ is chosen.

The LSSVR model obtained from [13] is shown below:

$$f(\mathbf{x}) = \sum_{i=1}^{m} \alpha_i K\left(\mathbf{x}_i, \mathbf{x}\right) + b \tag{8}$$

where α_i is the Lagrange multiplier, and b is the bias term.

Finally, LSSVR is used to calculate the response values of all sampling points in the exhaustive sampling set $\mathbf{S}_1$, generating a simulation result set $\mathbf{Y}_{\mathrm{LSSVR}}$ based on LSSVR. A statistical analysis is then performed on this set to obtain uncertainty analysis results.

3. FAILURE RATE OF EMC UNCERTAINTY ANALYSIS

The purpose of the EMC uncertainty analysis method is to calculate the propagation of uncertainty from input to output parameters. When the input parameters of an EMC simulation are uncertain due to real-world non-idealities, this uncertainty is also reflected in the output. As shown in the simulation results in Figure 1, any given point on a one-dimensional curve represents not just a value, but a range of values or a probability density function (PDF). The uncertainty in the output results introduces the potential for system failure. In practical engineering, many precision instruments have stringent electromagnetic compatibility requirements. If the output uncertainty exceeds the electromagnetic compatibility threshold, the system may be at risk of failure.

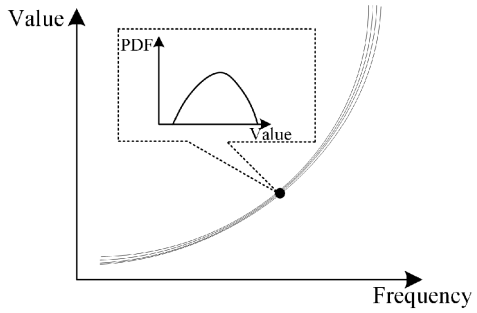

FIGURE 1. Result of the EMC uncertainty analysis.

The failure domain refers to the portion of the EMC uncertainty output that represents failure. This article uses PDF curves to characterize the failure domain from two perspectives of EMC. EMC encompasses two key requirements. On one hand, it refers to the requirement that the electromagnetic interference generated by a device during normal operation does not exceed certain limits within its environment, i.e., EMC disturbance. On the other hand, it involves the requirement that a device has a certain level of immunity to the electromagnetic interference present in its environment, i.e., EMC immunity.

Figure 2 presents a schematic diagram of the failure domain. From the perspective of EMC disturbance, system failures caused by excessive electromagnetic interference from the device, such as crosstalk in the cable bundle, are considered.

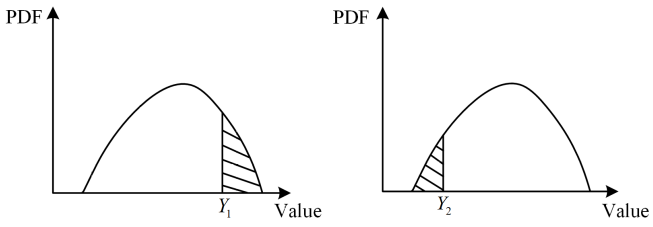

FIGURE 2. Failure domain for EMC uncertainty analysis.

The failure domain is defined as the area above the critical interference threshold, as shown below:

$$F = \{\mathbf{X} : Y(\mathbf{X}) > Y_1\} \tag{9}$$

where $\mathbf{X}$ is the EMC uncertainty input, Y the system output, and Y_1 the critical failure threshold.

From the perspective of EMC immunity, system failures are caused by equipment's inability to meet immunity standards, such as the shielding effectiveness of metal boxes. The failure domain is an area where the critical immunity threshold is exceeded, as shown below:

$$F = \{\mathbf{X} : Y(\mathbf{X}) < Y_2\} \tag{10}$$

where $\mathbf{X}$ is the EMC uncertainty input, Y the system output, and Y_2 the critical failure threshold.

Failure rate is the proportion of points in the failure domain to the entire sample space. The concept of failure rate is more clearly illustrated in this paper with the help of the PDF curve, as shown in Equation (11).

$$P_r = \int_F \mathrm{pdf}(\varepsilon) d\varepsilon \tag{11}$$

where $\mathrm{pdf}(\varepsilon)$ is the probability density function.

Credibility assessment is used to compare the results of the uncertainty analysis with reference data to verify the accuracy of the EMC uncertainty analysis method. This article proposes the concept of failure rate and uses it in the next section to assess the credibility of the uncertainty analysis method.

4. EXAMPLE ANALYSIS

This article presents the metal box shielding effectiveness example to evaluate the performance of the failure rate and discusses the results of the credibility assessment based on both the failure rate and MEAM.

Metal boxes are commonly used to shield against electromagnetic radiation. Holes are punched in their surface to allow the passage of power lines or for heat dissipation, which can reduce the overall shielding effectiveness. The size of these apertures is influenced by manufacturing tolerances or corrosion, which are often random. Uncertainty in the aperture size can impact the shielding effectiveness. If the shielding effectiveness falls below the critical failure threshold, the shielding effectiveness of the metal box is deemed to fail.

4.1. Example of a Single-Hole Metal Box Based on the Robinson Method

Robinson method [15] is an analytical algorithm used to predict the shielding effectiveness of an open-hole shielded box. It is simple in form and fast in calculation. However, it can only accurately calculate the shielding effectiveness of a single-hole metal box. In this study, the Robinson method is applied to calculate the shielding effectiveness of the single-hole metal box shown in Figure 3.

The rectangular metal box has a cavity with internal dimensions $a \times b \times d$, thickness t, and a rectangular aperture in the center of the panel with dimensions $l \times w$. There is excitation

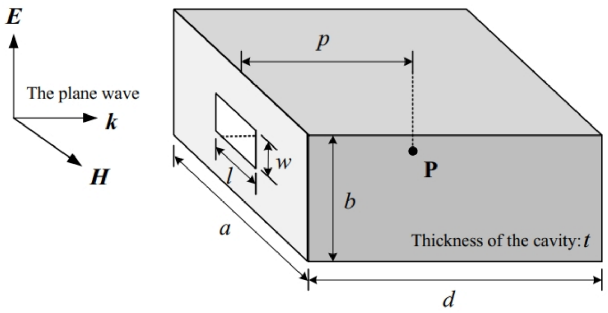

FIGURE 3. Schematic diagram of a single-hole metal box shielding effectiveness example.

plane wave radiation outside the metal box, which is incident on the rectangular cavity face of the opening perpendicular to the panel and polarized along the height of the cavity. The shielding effectiveness test point **P** is along the center of the panel at a distance p from the open aperture. The specific values of the partial parameters are $a = 300\,\text{mm}$, $b = 120\,\text{mm}$, $d = 300\,\text{mm}$, $t = 1\,\text{mm}$, and $p = 150\,\text{mm}$. The metal chosen is aluminum, which has a conductivity of $\sigma = 3.8 \times 10^7\,\text{S/m}$ and a relative permittivity of $\varepsilon_r = 1$. The rest of the solution space is similarly approximated as a vacuum.

It is assumed that the length l and width w of the rectangular aperture in the center of the panel are the uncertainty factors for this example, described by the following random variables:

$$\begin{cases} l = 100 + 10 \times \xi_1\,[\text{mm}] \\ w = 5 + 0.5 \times \xi_2\,[\text{mm}] \end{cases} \tag{12}$$

where ξ_1 and ξ_2 are uniformly distributed random variables in the interval $[-1, 1]$.

According to Robinson method, it is assumed that the frequency of the excitation plane wave is $f = 40\,\text{MHz}$. The value of the electric field strength at point **P** in the absence of a metal box is calculated as E_0. The value of the electric field strength at point **P** in the presence of a metal box is calculated as E_1. The result of the shielding effectiveness at this frequency point is shown below:

$$S_E = 20 \times \log_{10}\left(\frac{E_0}{E_1}\right)\,[\text{dB}] \tag{13}$$

The results of the uncertainty analyses of the MCM are used as standard data, which are performed for 10,000 deterministic simulations at the exhaustive sampling point S_1 to ensure convergence. The sample space S_2 of Kriging and LSSVR has 36 sampling points, i.e., $m = 36$. Deterministic simulations are performed on these sampling points to obtain the training set, which in turn leads to the construction of the surrogate model and finally produces the results of the uncertainty analysis. Figure 4 illustrates the PDF curves for MCM, Kriging, and LSSVR.

The shielding effectiveness requirements for metal boxes vary based on the application. According to the standards in [16], it is assumed that the shielding box used in this study is a "general" electromagnetic shielding box, with a shielding

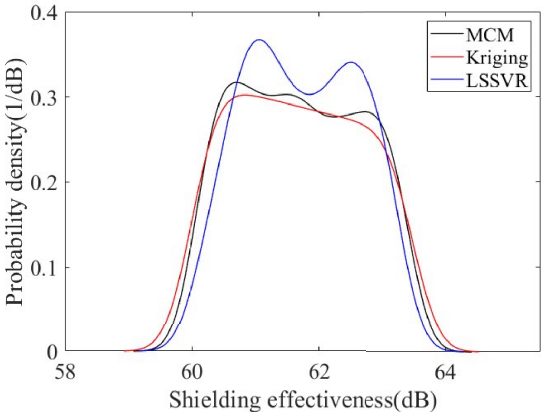

FIGURE 4. Probability density of the shielding effectiveness of a single-hole metal box.

index requirement of $S_E > 60\,[\text{dB}]$. In other words, the failure domain of the shielding effectiveness of the metal box is:

$$F = \{\mathbf{X} :\ S_E(\mathbf{X}) < 60\,[\text{dB}]\} \tag{14}$$

Figure 5 shows the shielding effectiveness failure domain based on three uncertainty analysis methods. MCM has extremely high calculation accuracy and is a widely recognized reference standard in the field of EMC simulation [17]. Therefore, the closer the result obtained by other uncertainty analysis methods is to that of the MCM, the higher the accuracy of the method is.

The shielding effectiveness failure rate results based on the three uncertainty analysis methods are shown in Table 1. The failure rate $P_{r(\text{MCM})}$ of MCM is 1.22%, which is used as the standard. The failure rate $P_{r(\text{Kriging})}$ of Kriging is 1.36%, and its relative error is 11.48%. The failure rate $P_{r(\text{LSSVR})}$ of LSSVR is 0.95%, and the relative error is 22.13%. A relative error of 10% is considered to be one order of magnitude. It can be seen that when the reliability is assessed using the failure rate, the accuracies of Kriging and LSSVR are relatively high, differing by only one order of magnitude, with Kriging being slightly more accurate than LSSVR.

TABLE 1. Failure rate results.

	failure rate	relative error
MCM	1.22%	/
Kriging	1.36%	11.48%
LSSVR	0.95%	22.13%

The MEAM results of the two uncertainty analysis methods, Kriging and LSSVR, are shown in Table 2. The MEAM result of Kriging is 0.9762, and the MEAM result of LSSVR is 0.8977. The MEAM assessment result is a constant between 0 and 1. The closer the value is to 1, the smaller the difference is, and the more accurate the uncertainty analysis method is [11].

TABLE 2. MEAM result.

	MEAM
Kriging	0.9762
LSSVR	0.8977

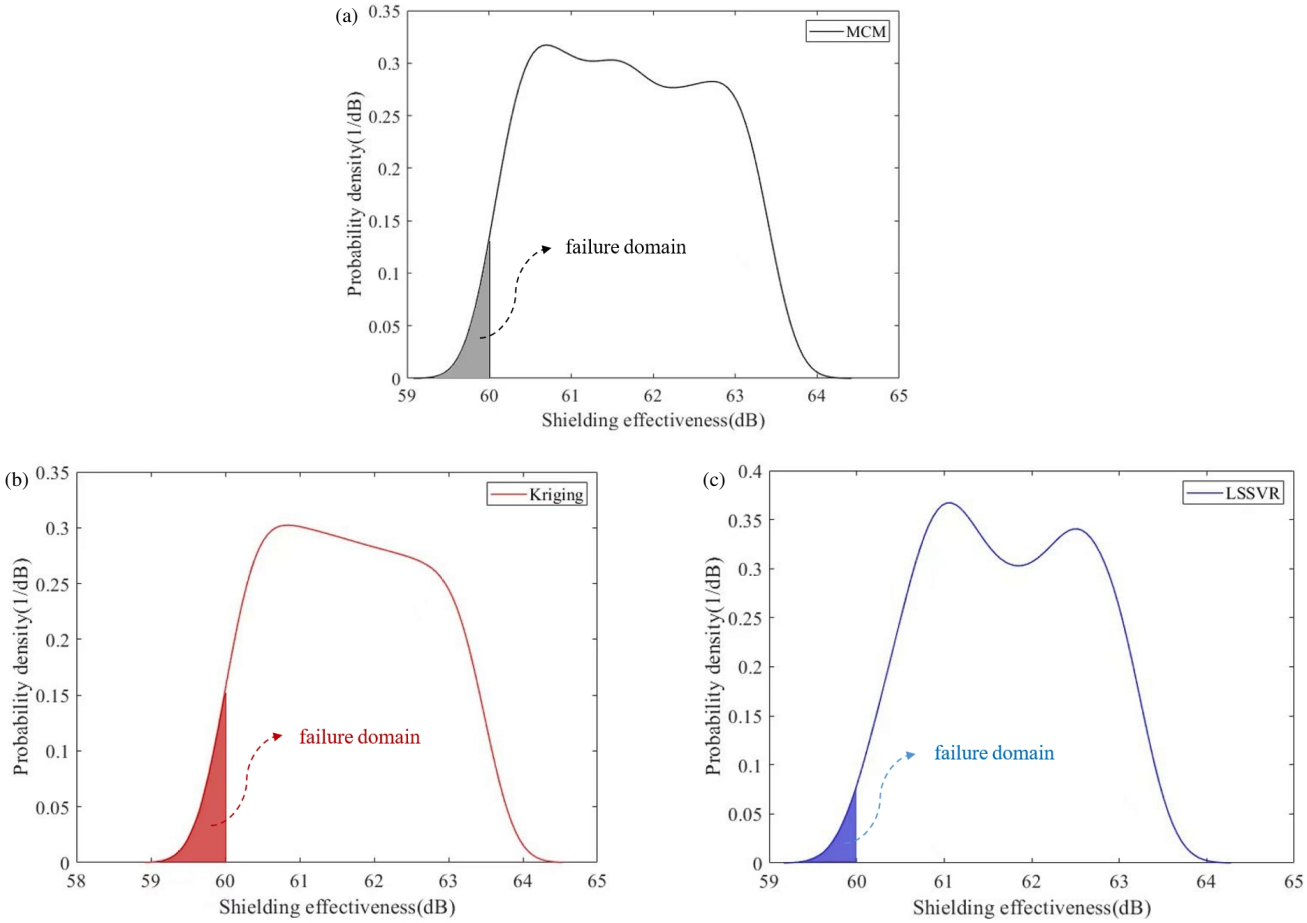

FIGURE 5. Shielding effectiveness failure domain based on three uncertainty analysis methods. (a) MCM, (b) Kriging, (c) LSSVR.

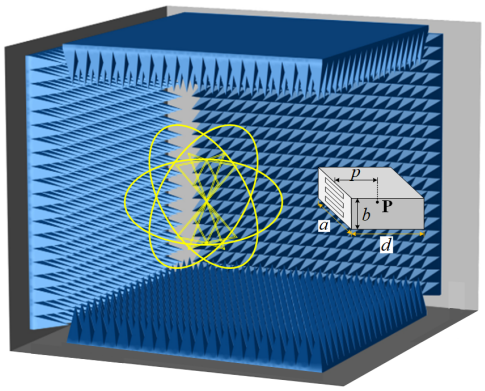

FIGURE 6. Schematic diagram of the shielding effectiveness example for a perforated metal box.

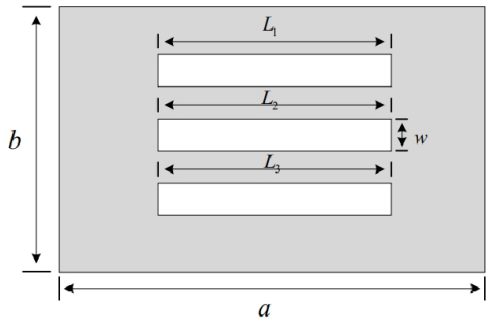

FIGURE 7. Schematic diagram of the apertures of the three-aperture metal box.

Therefore, when MEAM is used for credibility assessment, the accuracy of Kriging is slightly higher than that of LSSVR. The failure rate assessment result is consistent with that of MEAM.

4.2. Porous Metal Box Example Based on the Finite Element Method

To further test the performance of the failure rate, this section constructs a perforated metal box model using COMSOL simulation software. As shown in Figure 6, an anechoic chamber is first constructed to absorb electromagnetic waves inside and block incoming signals from outside. Then, a biconical antenna is placed at the center of the chamber to emit electromagnetic waves. Finally, a three-hole metal box is built at a certain distance from the antenna.

The metal box parameters in this example are the same as those in the previous section, except for the parameters of the apertures. The internal dimensions of the cavity of the rectangular metal box are $a \times b \times d$, where $a = 300$ mm, $b = 120$ mm,

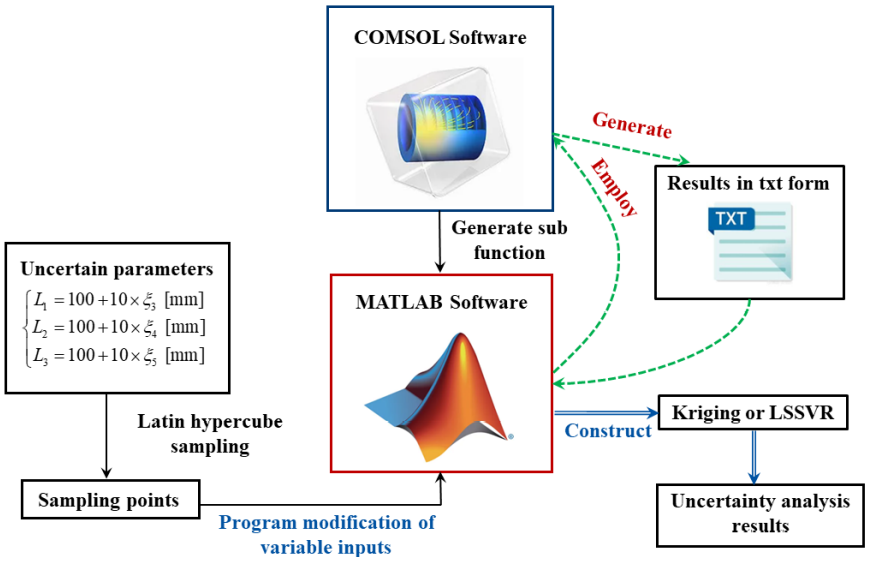

FIGURE 8. Construction of joint simulation platform of MATLAB software and COMSOL software.

$d = 300$ mm, and thickness $t = 1$ mm. The shielding effectiveness test point **P** is along the center of the panel at a distance $p = 150$ mm from the aperture. The metal chosen is aluminum, which has a conductivity of $\sigma = 3.8 \times 10^7$ S/m and a relative permittivity of $\varepsilon_r = 1$, and the rest of the solution space is similarly approximated as a vacuum. The parameters of the apertures are shown in Figure 7, and the lengths of the three apertures are L_1, L_2, and L_3. The widths of the apertures are all $w = 5$ mm.

It is assumed that L_1, L_2, and L_3 are the uncertainty factors for this example, described by the following random variables:

$$\begin{cases} L_1 = 100 + 10 \times \xi_3 \text{ [mm]} \\ L_2 = 100 + 10 \times \xi_4 \text{ [mm]} \\ L_3 = 100 + 10 \times \xi_5 \text{ [mm]} \end{cases} \tag{15}$$

where ξ_3, ξ_4, and ξ_5 are uniformly distributed random variables in the interval $[-1, 1]$.

To ensure the realization of the uncertainty analysis, this example requires the joint simulation of COMSOL and MATLAB software. The construction process of the joint simulation platform is shown in Figure 8. First, based on the uncertainty parameter in Equation (15), Latin hypercube sampling is applied to obtain the sampling points (S_2). The number of sampling points in this example is the same as in the previous section of the example, i.e., $m = 36$. The metal box model built in COMSOL is converted into MATLAB subfunctions, allowing MATLAB to call COMSOL for finite element simulation. Random variable inputs are modified based on the sampling points. After the necessary preparation, MATLAB and COMSOL are linked. MATLAB calls COMSOL to perform deterministic EMC simulations at the sampling points, and the generated simulation results are saved in a TXT file. MATLAB then constructs the Kriging model or LSSVR model by accessing the data in the TXT file. Finally, the uncertainty analysis results are obtained by substituting the exhaustive sampling points S_1 into the surrogate model. Notably, this example is also simulated at

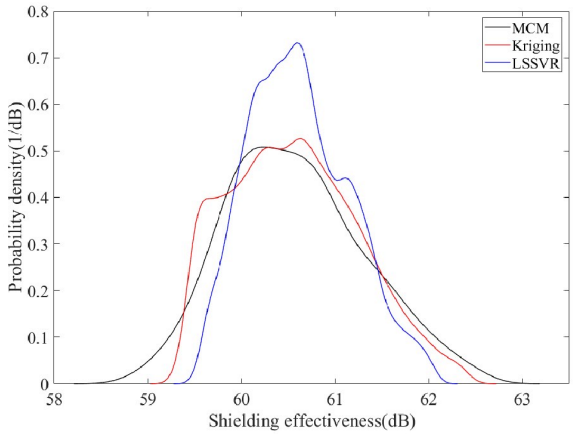

FIGURE 9. Probability density of the shielding effectiveness of the perforated metal box.

frequency ($f = 40$ MHz) to calculate the shielding effectiveness (S_E) at point (**P**). Moreover, the MCM performs 10,000 deterministic simulations at the exhaustive sampling points S_1, which are used as reference data.

Figure 9 shows the probability density curves for the three uncertainty analysis methods. The critical failure threshold for this example is also set to 60 [dB], which is consistent with the example in the previous section.

The failure rate of the shielding effectiveness of the perforated metal box is shown in Table 3. The failure rate $P_{r(\text{MCM})}$ of MCM is 22.80%, which is used as the standard. The failure rate $P_{r(\text{Kriging})}$ of Kriging is 23.88%, and its relative error

TABLE 3. Failure rate results.

	failure rate	relative error
MCM	2280%	/
Kriging	2388%	4.74%
LSSVR	12.59%	44.78%

is 4.74%. The failure rate $P_{r(\mathrm{LSSVR})}$ of LSSVR is 12.59%, and the relative error is 44.78%. When the failure rate is used for credibility assessment, the relative error of LSSVR is four orders of magnitude higher than that of Kriging, making Kriging significantly more accurate than LSSVR. Table 4 presents the MEAM results, which indicate that Kriging is more accurate than LSSVR. The failure rate results align with the MEAM results, both showing that Kriging is more accurate than LSSVR. However, from the perspective of failure rate assessment, the accuracy gap between Kriging and LSSVR is even wider, with Kriging being significantly more accurate than LSSVR.

TABLE 4. MEAM result.

	MEAM
Kriging	0.9356
LSSVR	0.7340

5. DISCUSSION ON FUTURE RESEARCH WORK

In the EMC uncertainty analysis study, the next step of the study focuses on determining the convergence of the sample points. In the subsequent study, a method for determining the convergence of uncertainty based on mechanical tolerances and failure rates will be proposed, and the failure rates will be further investigated based on the measurement uncertainty.

6. CONCLUSION

This article proposes a credibility assessment method for EMC uncertainty analysis based on failure rate, focusing on the practical application of uncertainty analysis methods. Uncertainty analysis based on Kriging and LSSVR is applied to the example of metal box shielding effectiveness, and the results are evaluated using the failure rate to assess the accuracy of the two methods in practical applications. Finally, the failure rate-based assessment results are compared with those of the classical MEAM, and it is found that the two methods yield consistent results. Furthermore, the failure rate-based method focuses more on the performance of different uncertainty analysis models in the failure domain, making it more accurate than the MEAM, which considers the entire system when assessing system failure. This article provides a theoretical reference for uncertainty analysis methods to guide practical electromagnetic compatibility design.

ACKNOWLEDGEMENT

This paper is supported by "The Open Fund of National Center for International Research of Subsea Engineering Technology and Equipment" (Project No. HG20240201).

REFERENCES

[1] IEEE Standard Association, "IEEE Standard for Validation of Computational Electromagnetics Computer Modeling and Simulations," *IEEE Std. 1597.1-2008*, 1–41, 2008.

[2] IEEE Standard Association, "IEEE Recommended Practice for Validation of Computational Electromagnetics Computer Modeling and Simulations," *IEEE Std.1597.2-2010*, 1–124, 2011.

[3] Orlandi, A., G. Antonini, C. Polisini, A. Duffy, and H. Sasse, "Progress in the development of a 2D feature selective validation (FSV) method," in *2008 IEEE International Symposium on Electromagnetic Compatibility*, 1–6, Detroit, MI, USA, Aug. 2008.

[4] Zhang, G., A. P. Duffy, H. Sasse, L. Wang, and R. Jauregui, "Improvement in the definition of ODM for FSV," *IEEE Transactions on Electromagnetic Compatibility*, Vol. 55, No. 4, 773–779, Aug. 2013.

[5] Zhang, G., A. P. Duffy, A. Orlandi, D. D. Febo, L. Wang, and H. Sasse, "Comparison of data with multiple degrees of freedom utilizing the feature selective validation method," *IEEE Transactions on Electromagnetic Compatibility*, Vol. 58, No. 3, 784–791, Jun. 2016.

[6] IEEE Standard Association, "IEEE Standard for Validation of Computational Electromagnetics Computer Modeling and Simulations," *IEEE Std. 1597.1-2022*, 1–52, 2022.

[7] Bai, J., Y. Wan, M. Li, G. Zhang, and X. He, "Reduction of random variables in EMC uncertainty simulation model," *Applied Computational Electromagnetics Society Journal (ACES)*, Vol. 37, No. 9, 941–947, Sep. 2022.

[8] Tan, T., T. Jiang, H. Jiang, T. Wang, and M. Cai, "Uncertainty quantification method of crosstalk involving braided-shielded cable," *Applied Computational Electromagnetics Society Journal (ACES)*, Vol. 38, No. 1, 28–35, Jan. 2023.

[9] Jauregui, R., M. Aragon, and F. Silva, "The role of uncertainty in the feature selective validation (FSV) method," *IEEE Transactions on Electromagnetic Compatibility*, Vol. 55, No. 1, 217–220, Feb. 2013.

[10] Ferson, S., W. L. Oberkampf, and L. Ginzburg, "Model validation and predictive capability for the thermal challenge problem," *Computer Methods in Applied Mechanics and Engineering*, Vol. 197, No. 29-32, 2408–2430, May 2008.

[11] Bai, J., L. Wang, D. Wang, A. P. Duffy, and G. Zhang, "Validity evaluation of the uncertain EMC simulation results," *IEEE Transactions on Electromagnetic Compatibility*, Vol. 59, No. 3, 797–804, Jun. 2017.

[12] Bai, J., G. Zhang, D. Wang, A. P. Duffy, and L. Wang, "Performance comparison of the SGM and the SCM in EMC simulation," *IEEE Transactions on Electromagnetic Compatibility*, Vol. 58, No. 6, 1739–1746, Dec. 2016.

[13] Trinchero, R., M. Larbi, H. M. Torun, F. G. Canavero, and M. Swaminathan, "Machine learning and uncertainty quantification for surrogate models of integrated devices with a large number of parameters," *IEEE Access*, Vol. 7, 4056–4066, 2018.

[14] Han, Z.-H. and S. Görtz, "Hierarchical kriging model for variable-fidelity surrogate modeling," *AIAA Journal*, Vol. 50, No. 9, 1885–1896, Sep. 2012.

[15] Robinson, M. P., T. M. Benson, C. Christopoulos, J. F. Dawson, M. D. Ganley, A. C. Marvin, S. J. Porter, and D. W. P. Thomas, "Analytical formulation for the shielding effectiveness of enclosures with apertures," *IEEE Transactions on Electromagnetic Compatibility*, Vol. 40, No. 3, 240–248, Aug. 1998.

[16] Chinese Standard, "GB/T 50719-2011, Technical code for electromagnetic shielded enclosure."

[17] Bai, J., K. Guo, J. Sun, and N. Wang, "Application of the multi-element grid in EMC uncertainty simulation," *Applied Computational Electromagnetics Society Journal (ACES)*, Vol. 37, No. 4, 428–434, Apr. 2022.